
Out-of-Distribution Generalization with Maximal Invariant Predictor

Masanori Koyama *
Preferred Networks
Tokyo, Japan
masomatics@preferred.jp

Shoichiro Yamaguchi *
Preferred Networks
Tokyo, Japan
guguchi@preferred.jp

Abstract

Out-of-Distribution (OOD) generalization problem is a problem of seeking the predictor function whose performance in the worst environments is optimal. This paper makes two contributions to OOD problem. We first use the basic results of probability to prove *Maximal Invariant Predictor* (MIP) condition, a theoretical result that can be used to identify the OOD optimal solution. We then use our MIP to derive *Inter-environmental Gradient Alignment* (IGA) algorithm that can be used to help seek the OOD optimal predictor. Previous studies that have investigated the theoretical aspect of the OOD problem use strong structural assumptions such as causal DAG. However, in cases involving image datasets, for example, the identification of hidden structural relations is itself a difficult problem. Our theoretical results are different from those of many previous studies in that it can be applied to cases in which the underlying structure of dataset is difficult to analyze. We present an extensive comparison of previous theoretical approaches to the OOD problems based on the assumptions they make. We also present an extension of the Colored-MNIST that can more accurately represent the pathological OOD situation than the original version, and demonstrate the superiority of IGA over previous methods on both the original and the extended version of Colored-MNIST.

1 Introduction

In general, most machine learning algorithms today make an inherent assumption that all members of all datasets in concern are independently and identically sampled from the same distribution (IID) [5]. Unfortunately, this assumption is not always valid [5]. In reality, train-dataset and test-dataset can be coming from different distributions, on which the input-output relations are different because of the presence of environmental factors such as those related to the way the data were collected and where the data were obtained [33, 35]. This is why most machine learning algorithms often fail when challenged to make prediction on the dataset sampled from “yet-unseen” distribution (“out of distribution (OOD)” dataset). To address this problem, we need to consider the set of distributions that can be produced by all possible environmental factors, and look for the model whose worst-case performance is optimal; that is, we want to find a solution of

$$\arg \min_f \max_{\epsilon \in \mathcal{A}} \text{Cost}(f|\epsilon) \quad (1)$$

where \mathcal{A} is the set of all possible values for the environmental factors, and $\text{Cost}(f|\epsilon)$ is the cost of the model f in the presence of the environmental factor ϵ . The problem (1) is often referred to as *OOD* generalization problem [1, 7]. We would say that f is OOD-optimal if it solves (1). Unfortunately, as mentioned in [1], the problem (1) often cannot be directly optimized because we cannot observe all datasets in all environments. This dilemma gives rise to the following two questions that must be

*Equal contribution

answered, in the following order: **(I) Is there any tractable necessary/sufficient condition for the OOD optimality?** **(II) Is there any algorithm that can seek the solution to the OOD problem?**

All the works that tackled the question (I) differ by the assumptions they make about the following three items: (i) data generation process, (ii) invariance type, and (iii) model complexity. By *Data generation process*, we mean the way the outputs are generated from the input. Causal DAG, for example, is one description of data generation process [29, 36]. *Invariance type* describes the part of $P(Y, X|\epsilon)$ that is assumed to be invariant with respect to ϵ . Indeed, if we assume that any distribution can be constructed by some environmental factor ϵ , the OOD problem (I) would have degenerate solutions. Covariate shift, for example, assumes $P(Y|X, \epsilon) = P(Y|X)$ irrespective of the choice of ϵ [3, 34]. The recent work of [1] assumes that there exists a feature $\Phi(X)$ with $\mathbb{E}[Y|\Phi(X), \epsilon] = \mathbb{E}[Y|\Phi(X)]$. Finally, *Model complexity* is about the sheer complexity of the Input/Output relation. However, in general, validating these structural assumptions is itself a difficult problem that can require massive computation resources [7, 29]. For image recognition, for example, it is unrealistic to seek the causal DAG that governs the relationships among all pixels and the label. However, as we discuss in section 2.1, there has not been a study that has theoretically analyzed the OOD optimality problem in such situations. As a theoretical work that can be used to discuss the OOD optimality on datasets with intractable underlying structure, our work is the first of its kind.

On the other hand, all OOD algorithms that aim to solve (II) differ by the amount of the prior knowledge about the following two items they use in their procedures: *underlying structure of the model* and *the type of the dataset*. [29, 36], for example, directly use the topology of the causal network in their algorithms. [30] assumes that all useful features can be extracted using discrete mask functions. Again, however, these prior knowledges are not always readily available in practice [7, 29].

To develop a theory and an algorithm that can be applied to situations in which the underlying structure is difficult to identify, we tackle the question (I) while only assuming that there exists at least one feature $\Phi(X)$ for which $P(Y|\Phi(X), \epsilon) = P(Y|\Phi(X))$ (assumption(ii)). As our partial answer to the question (I), we present a sufficient condition for the OOD solution in the form of Maximal Invariant Predictor (MIP) condition, a requirement described in the language of mutual information. As our answer to the question (II), we derive Inter-environmental Gradient Alignment (IGA) algorithm from MIP. Like [1], our IGA requires no prior knowledge about the model structure and the type of dataset. To demonstrate the efficacy of IGA, we conduct experiments on an extended version of Colored-MNIST [1] that can be used to more accurately construct the pathological OOD situation described in [1]. We also extensively compare the contemporary OOD studies in terms of the assumptions they use in their approach to (I) and (II). We summarize our contributions below.

- We prove several theoretical statements about the OOD optimality and present MIP, a condition that can guarantee the OOD optimality under an appropriate set of conditions. We achieve this
 1. without using the language of causality (assumption (i)),
 2. without making any stronger invariance assumption than the presence of *invariant predictor* (a feature $\Phi(X)$ for which $P(Y|\Phi(X), \epsilon) = P(Y|\Phi(X))$) (assumption (ii)),
 3. without making any assumption about the complexity of the model (assumption (iii)).
- We propose Inter-environmental Gradient Alignment algorithm that can be used to seek a solution that satisfies the MIP condition.
- We present an extended version of Colored-MNIST [1] that can be used to more accurately describe the pathological OOD situation introduced in the original article, and demonstrate the efficacy of IGA on both extended Colored-MNIST and the original Colored-MNIST.

Our paper is structured as follows. In the next section, we describe the set of assumptions we use for the problem (I) more formally, and present an extensive comparison of how the previous works approached the problem (I). In section 3, we present our solution to (I) along with the related theoretical results. In section 4, we present our solution to (II) and describe IGA. Finally, in section 5, we demonstrate the efficacy of IGA on MNIST-derived datasets.

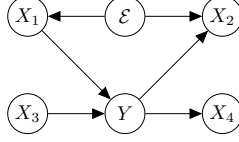


Figure 1: A graphical model with nonempty \mathcal{I} (eq (3)). The target variable is Y and the covariate is $X := [X_1, X_2, X_3, X_4]$.

2 Problem Setting for the OOD optimality problem (for question (I))

In this section, we introduce the set of notations we use throughout the paper, and describe our question (I) in more formal language. We use r.v to abbreviate *random variable*.

Notation We follow the rules of notations used in a standard probability text like [11]. For any set of r.vs $\mathcal{M} = \{M_1, M_2, \dots\}$ on the probability triple (Ω, \mathcal{F}, P) , we say $Z \in \sigma(\mathcal{M})$ or Z is *measurable with respect to* $\sigma(\mathcal{M})$ whenever Z can be written as a measurable function of M s. **We may use Z and $Z(M)$ interchangeably in this case**². We say $A \perp B$ when A and B are independent. Also, let Z^c denote an independent complement of Z in M for which $Z^c \perp Z$ and $M \in \sigma(Z^c, Z)$ ³. Let us also use a lower case letter to denote a realization of the corresponding r.v (m is a realization of M , and ϵ is a realization of \mathcal{E}). We always use \mathbb{E} to represent the expectation with respect to the probability distribution P . Inside \mathbb{E} , variables in upper case are the only variables that are integrated with respect to P . Also, for any probability distribution Q on \mathcal{F} , we use its lower case q to denote its density. In what follows, we will use these formal definitions to rephrase the problem (I) along with the set of assumptions.

Formal Problem Statement Let X, Y, \mathcal{E} respectively represent the input r.v, the target r.v, and the environmental r.v. At the time of the training, only X, Y are observable, and the observations are only grouped by the realizations of \mathcal{E} . We will measure the performance of the predictor $f(X)$ by Bregman divergence loss D , which generalizes popular losses like KL divergence and Mean Square Error [2]. That is, for all $\epsilon \in \text{supp}(\mathcal{E})$, we compute the loss on environment ϵ by $L_\epsilon(f) := \mathbb{E}[D(f(X), Y)|\epsilon]$. The OOD problem is to seek the minimizer of the Out-of-Distribution (OOD) loss, given by

$$\arg \min_f \max_{\epsilon \in \text{supp}(\mathcal{E})} L_\epsilon(f), \quad (2)$$

We say that f is OOD optimal if it is a solution to (2). As our partial answer to the problem (I), we derive a set of necessary conditions for the OOD optimal solution under the following assumptions about (i) data generation process, (ii) invariance type, and (iii) model complexity.

(i) Data generation Process We assume that data is generated from an abstract distribution $P(X, Y, \mathcal{E})$. In particular, we do not assume that we have a decomposition of X that is adapted to some underlying causality relations [29, 36].

(ii) Invariance type We assume that

$$\mathcal{I} := \{\Phi \in \sigma(X); Y \perp \mathcal{E}|\Phi\} = \{\Phi \in \sigma(X); I(Y; \mathcal{E}|\Phi) = 0\} \quad (3)$$

is non-empty. We refer to \mathcal{I} as the set of *invariant predictors* from now on. In the graphical model represented in Figure 1, for example, \mathcal{I} is the set of all random variables that can be constructed from some subset of $\{X_1, X_3, X_4\}$ that contains X_1 . This fact can be verified with d-separation theorem [6]. Our invariance assumption is not too far-fetched. For example, consider the problem of animal-image recognition. If Y, X, \mathcal{E} are respectively the animal label, the image, and the person who takes the picture, an animal's biological feature captured in the image is a member of \mathcal{I} . Indeed, such Φ is not unique all the time; for instance, *face of animal* itself might be in \mathcal{I} . This is also the case for the graphical model in Figure 1.

(iii) Model complexity We only assume that all functions to appear in our analysis fulfill the appropriate set of regularity conditions (continuity, differentiability, etc.) that are required to make each statement in our theory valid.

²For those not familiar with this notation, please identify $\sigma(M)$ as $\{Z; Z = g(M) \text{ for some function } g\}$ in the main part of this manuscript.

³Such a complement exists when the cumulative distribution function of M given Z is sufficiently regular (more precisely, measurable as a function of Z [10]).

Reference	(i) Data generation process	(ii) Invariance type	(iii) Model complexity	OOD optimality guarantee
[7, 29, 31]	entire DAG	$Y \perp \mathcal{E} \Phi$	Linear	Yes
[25, 36]	entire DAG	$Y \perp \mathcal{E} \Phi$	Non-Linear	Yes
[30]	DAG node set	$Y \perp \mathcal{E} \Phi$	Linear & Non-Linear	Yes
[3, 19, 34]	Unknown	$Y \perp \mathcal{E} X$	Non-Linear	Yes†
[21, 38]	Unknown	$\Phi \perp \mathcal{E}$	Non-Linear	Unknown‡
[22, 23]	Unknown	$\Phi \perp \mathcal{E} Y$	Non-Linear	Unknown
[1]	Unknown	$\mathbb{E}[Y \Phi] = \mathbb{E}[Y \Phi, \mathcal{E}]$	Non-Linear	Unknown
Ours	Unknown	$Y \perp \mathcal{E} \Phi$	Non-Linear	Yes

Table 1: Previous studies of OOD problem categorized by the types of assumption-settings. The dagger sign indicates that, with an appropriate set of additional assumptions, the OOD optimality of the corresponding method can be guaranteed using our theory (section 3).

2.1 Problem settings used in other OOD studies

A part of the novelty of our theoretical work is the generality of assumptions under which we tackle the question (I). Before we present our answer to the question (I), we therefore describe the assumption-settings used by other works. Table 1 compares the approaches of previous works in terms of the assumptions they make about (i) data generation process, (ii) invariance type, and (iii) the model complexity. The methods that come with the guarantee of the OOD optimality are labeled *Yes* in the right-most column. Below, we explain the assumptions of the previous works in more detail.

(i) Data generation process Many works assume that the underlying model can be represented by causal DAG, and use DAG definitions to discuss the OOD optimality [29, 36, 30, 7]. We therefore categorized the assumption about the data generation process by the amount of DAG information used in the analysis. In Table 1, we used the label *entire DAG* to designate the studies that use the DAG network to discuss the OOD optimality, and used the label *DAG node set* to designate the methods that only used the node-set of DAG. Finally, we used the label *unknown* to designate the studies that did NOT use the language of DAG [1, 3, 21, 34].

(ii) Invariance type Causal DAG based approaches [7, 29, 30, 36] practically assume the presence of at least one invariant predictor (i.e. Φ with $Y \perp \mathcal{E} | \Phi$). In this family of methods, it is assumed that the distribution of each node variable X is governed by the set of parent variables, $Pa(X)$. In this setting, the natural strategy is to find good members of $Pa(Y)$ whose relation to Y does not change by the environmental factor. These members of $Pa(Y)$ serve as Φ in Causal DAG based methods [7]. Covariate shift [3, 19, 34] assume that $P(Y | X, \epsilon)$ is invariant with respect to ϵ . IRM [1], on the other hand, assumes the presence of Φ for which $\mathbb{E}[Y | \Phi, \mathcal{E}] = \mathbb{E}[Y | \Phi]$. This assumption is indeed weaker than ours. However, [1] focuses on the question (II) in their study, and does not provide their answers to (I) when the model is non-linear. Also, Adversarial Domain Adaption (ADA) [21, 37] uses discriminator to look for a feature Φ that is independent from ϵ (i.e. $\Phi \perp \mathcal{E}$), and uses $P(Y | \Phi)$ to predict the target variable Y . Our theory in next section shows that ADA solution can be OOD optimal if we can additionally assume that their feature Φ is also an invariant predictor. For example, such a case can occur in models like Colored-MNIST [1] in Section 5.1.

(iii) Model complexity Because the optimal solution of the loss function derived from a Bregman-type divergence often takes the form of conditional expectation [2], the OOD problem tends to become simpler when the model is linear and the conditional expectation can be evaluated easily. Thus, several methods approached the problem (I) under the linearity assumption [29, 30]. We, therefore, categorized the model complexities of previous methods by the linearity of the assumed underlying model.

Note that the set of assumptions we use for the problem (I) is weaker than those of most previous methods. Unlike many, we do not make specific assumptions about the model $P(Y, X | \epsilon)$ that generates the dataset. Our invariance assumption is relatively weak, and the assumptions of DAG based approaches and Covariate shift are both special cases of our assumption. More importantly, the set of cases we consider in our theoretical work contains cases that have not been considered in previous studies of OOD optimality. For example, we can apply our theory to the dataset involving images, in which neural nets is the only reasonable choice to model the input-output relations. Such cases are difficult to analyze with causality based methods. Unlike Covariate shift, our theory can also be applied when $P(Y, X | \epsilon)$ varies across tasks (such cases are also extensively discussed in [1]).

Several additional remarks are in order here. First, even when the underlying model is causal, the strategy of seeking a subset of $Pa(Y)$ does not necessarily find the OOD optimal solution. For instance, in the Markov chain $\mathcal{E} \rightarrow X \rightarrow Y \rightarrow Z$, the conditional distribution $P(Y|Z, X, \mathcal{E})$ is invariant with respect to \mathcal{E} , and $[Z, X]$ is clearly a better invariant feature than $X = Pa(Y)$ for the prediction of Y . To our best knowledge, there has not been a study that proved the precise set of theoretical conditions under which the OOD optimal predictor can be constructed using $Pa(Y)$ only. In our setting, we also consider the members of \mathcal{I} that cannot be described as a set of interpretable variables. Also, When the loss function is derived from a Bregman-type divergence, the OOD optimality of Covariate shift method [19, 34] follows from the property of $\mathbb{E}[Y|X]$.

3 Theory (for question (I))

In this section, we will provide our answers to the question (I). The candidate of the OOD problem we propose in this study is of form $\mathbb{E}[Y|\Phi]$, with $\Phi \in \mathcal{I}$ (definition in the notation section). We will prove the condition to be imposed on Φ that would guarantee the OOD optimality of $\mathbb{E}[Y|\Phi]$. After deriving this condition, we will derive Maximal Invariant Predictor (MIP), a more tractable alternative condition for the OOD optimality. For the proofs of the statements in this section, see the Appendix. As promised, we will neither assume a system governed by a causal DAG, nor assume something about the complexity of the model. We will only assume that the set \mathcal{I} of invariant predictors is non-empty. To prepare, we will define several variables that can be derived from Φ . To be concise, we will provide intuitive definitions here, and leave the technical definitions in Appendix B.

- $\mathcal{E}_\psi \in \sigma(\mathcal{E})$, a part of \mathcal{E} that is independent of Φ
- $\mathcal{E}_\phi = \mathcal{E}_\psi^c$; that is, $\mathcal{E}_\phi \perp \mathcal{E}_\psi$ and $\mathcal{E} \in \sigma(\mathcal{E}_\phi, \mathcal{E}_\psi)$.

Put in other words, this is a decomposition of \mathcal{E} into the component that can affect Φ and the component that cannot. Also, let us denote Φ^c by Ψ . That is, $\Psi \perp \Phi$ and $X \in \sigma(\Phi, \Psi)$. Then the next two statement holds:

Proposition 3.1. *Let $\Phi \in \mathcal{I}$. Also, put $f^*(X) = \mathbb{E}[Y|\Phi]$ and suppose that, for all ϵ_ϕ there exists $\tilde{\epsilon}_\psi$ such that⁴ $X \perp Y | (\Phi, \epsilon_\phi, \tilde{\epsilon}_\psi)$ (eq (4)). Then $f^* = \arg \min_f \max_{\epsilon \in \text{supp}(\mathcal{E})} L_e(f)$.*

Corollary 3.2. *Suppose that \mathcal{E} admits an independence decomposition $(\mathcal{E}_\phi, \mathcal{E}_\psi)$. If there exists one $\tilde{\epsilon}_\psi$ for which $\Psi \perp Y | \tilde{\epsilon}_\psi$, then $\mathbb{E}[Y|\Phi]$ is OOD optimal.*

The corollary 3.2 follows directly from the proposition B.2. The condition of the corollary 3.2 practically states that, if the underlying model is appropriate, we just need one environment to satisfy (11) in order to guarantee the OOD optimality of Φ . Figure 1 in Appendix B is an example of a system in which the corollary 3.2 can hold. For a more intuitive scenario, consider another image recognition problem of predicting the animal label Y from the image X in the set of natural images that were collected with the loose directive of “take any pictures of a given list of animals”. Suppose that Φ is the physical appearance of the animal. Then the part of the environmental factor that can influence to Φ can be the biological state of the animal (\mathcal{E}_ϕ) (e.g. physical state, genetic feature). The part of the environmental factor that can *not* influence Φ can be, for example, the preference of the photographer (\mathcal{E}_ψ). Clearly, $\mathcal{E}_\psi \perp \Phi$. Meanwhile, Ψ , the complement of Φ , would be the background of the animal. Since the photographer does not have much choice for the individual animal to encounter, Ψ is independent of Φ if he/she is not so picky.

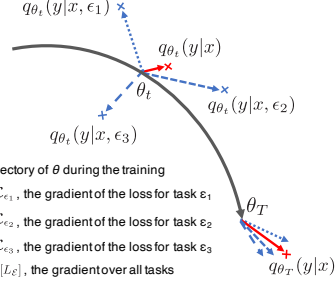
The corollary 3.2 may be helpful in determining when the OOD optimality statement in [30] is valid. In their proof, [30] claims their solution to be OOD-optimal under the assumption that, for any ϵ , there exists ϵ' such that $P(Y, X|\epsilon') = P(\Phi, Y|\epsilon)P(\Phi^c|\epsilon)$. Unfortunately, this does not hold in general. Also, as we stated in the previous section, the assumption that any joint distribution can be realized by some $\epsilon \in \text{supp}(\mathcal{E})$ can make the problem degenerate. However, we can guarantee the validity of their assumption if $\Psi \perp \mathcal{E}$ and if Φ satisfies the condition of the corollary 3.2. Now, is there any way to state the required condition for the relation eq(11) in Prop B.2 more concretely? Let us say that a given environment ϵ satisfies the **controllability condition** if there exists $\tilde{\epsilon}_\psi$ for which $X \perp Y | \epsilon_\phi, \tilde{\epsilon}_\psi$. It turns out that this relation holds only if Φ is the *best* predictor for at least one choice of ϵ ;

⁴As we describe in Appendix B, we can increase the number cases in which this holds if we choose \mathcal{E}_ψ to be larger in the sense of sigma algebra.

Algorithm 1 Inter-environmental Gradient Alignment Algorithm

Input: $q_\theta(y|x), \{D_\epsilon; \epsilon \in \mathcal{G}_{train}\}$
Return: q_θ
 1: **for** each iteration **do**
 2: **for** ϵ_i in \mathcal{G}_{train} **do**
 3: compute $L_{\epsilon_i}(\theta) = \mathbb{E}[\log q_\theta(Y|X)|\epsilon_i]$
 4: compute $\nabla_\theta L_{\epsilon_i}(\theta)$
 5: **end for**
 6: compute $\mathbb{E}[L_\mathcal{E}] := \frac{1}{|\mathcal{G}_{train}|} \sum_{\epsilon_i \in \mathcal{G}_{train}} L_{\epsilon_i}(\theta)$
 7: compute $\text{trace}(\text{Var}(\nabla_\theta L_\mathcal{E}(\theta))) := \sum_{\epsilon_i \in \mathcal{G}_{train}} \|\nabla_\theta L_{\epsilon_i}(\theta) - \nabla_\theta \mathbb{E}[L_\mathcal{E}]\|^2$
 8: update θ by the gradient descent using (6)
 9: **end for**

Table 2: IGA algorithm


 Figure 2: The relation of the θ -updates in IGA to the gradient computed at each task.

Proposition 3.3. Suppose $\Phi \in \mathcal{I}$ and suppose that ϵ^* satisfies the controllability condition Then for this ϵ^* , $\Phi = \arg \max_{Z \in \sigma(X)} I(Y; Z|\epsilon^*)$.

The situation considered here is not too unrealistic. In the case of the animal-recognition example we mentioned above, this can happen if ϵ_ψ^* is a person who wants to take a picture of every animal in front of an all-green background for the Chroma-key purpose. With such ϵ^* , the biological feature of an animal would always be the best feature. However, on its own, it is still difficult to verify when such a condition is satisfied. We, therefore, propose still another form of the requirement for Φ ;

Proposition 3.4. suppose that there exists ϵ^* that satisfies the controllability condition. Then there exists no $\tilde{\Phi} \in \mathcal{I}$ with $\Phi \in \sigma(\tilde{\Phi})$ such that $I(Y; \Phi) < I(Y; \tilde{\Phi})$.

3.1 Maximal Invariant Predictor

The proposition 3.4 states that, unless Φ is a maximal element of \mathcal{I} , there is no hope in finding an environment in which $\mathbb{E}[Y|\Phi]$ is OOD optimal. This motivates to find $\Phi \in \mathcal{I}$ satisfying

$$\Phi^* \in \arg \max_{\Phi \in \mathcal{I}} I(Y; \Phi) = \arg \max_{I(Y; \mathcal{E}|\Phi)=0} I(Y; \Phi). \quad (5)$$

We will refer this condition as *Maximal Invariant Predictor (MIP)* condition. Our MIP result provides justification to the hypothesis claimed in [12](blog). We can also make a little stronger statement when appropriate conditions are met. Note that, in cases like Figure 1, all invariant features are generated by a common invariant feature vector $[X_1, X_3, X_4]$. This type of case may also arise when the data is generated by undirected graphical model that is a perfect map [8](Appedix C). In these cases, MIP is unique and the proposition 3.4 would imply that Φ cannot be OOD optimal unless it achieves $\max_{\Phi \in \mathcal{I}} I(Y; \Phi)$. It turns out that, if we use these facts, we can claim the following:

Theorem 3.5. Suppose that \mathcal{I} can be generated by one invariant subset of r.v.s, and that there exists at least one $\Phi \in \mathcal{I}$ for which there is ϵ that satisfies the controllability condition. Then $\mathbb{E}[Y|\Phi]$ is OOD optimal if Φ is MIP.

4 Inter-environmental Gradient Alignment Algorithm (for question (II))

As our answer to the question (II), we present Inter-environmental Gradient Alignment (IGA), an algorithm to optimize the MIP objective. Table 2 is a summary of our algorithm. We use \mathbb{E} to denote the empirical expectation. Let $\mathcal{G}_{train} = \{\epsilon_1, \epsilon_2, \dots, \epsilon_k\} \subset \text{supp}(\mathcal{E})$ denote a size= k set of environments from which the user can collect the dataset. IGA assumes that the user is given a set of datasets $\{D_\epsilon; \epsilon \in \mathcal{G}_{train}\}$, with each D_ϵ being a set of samples from $p(y, x|\epsilon)$. Because we assume nothing about the *underlying model structure* and the *type of the dataset*, the identities and the effects of ϵ are not disclosed to the user in any way whatsoever. In the actual dataset, ϵ is only observable as an integer index of datasets. Now, if $q_\theta(y|x)$ is the prediction model and $L_\epsilon(\theta)$ is the prediction loss of $q_\theta(y|x)$ on D_ϵ , IGA seeks to optimize

$$\arg \min_{\theta} \mathbb{E}[L_\mathcal{E}(\theta)] + \lambda \text{trace}(\text{Var}(\nabla_\theta L_\mathcal{E}(\theta))). \quad (6)$$

4.1 Derivation of IGA

We derive (6) from the MIP objective (5). To evaluate $I(Y; \Phi)$ and $I(Y; \mathcal{E}|\Phi)$, we need to be able to evaluate both $p(y|\phi, \epsilon)$ and $p(y|\phi)$. However, the complexity of $p(y|\phi, \epsilon)$ is usually unknown. The relationship between $p(y|\phi, \epsilon)$ and $p(y|\phi)$ is unknown as well. To resolve this problem, we use specific parametrizations to represent these distributions. Note that because $\Phi \in \sigma(X)$ (so that Φ can be written as a function of X), $p(y|\phi)$ can be written as $q(y|x)$ for some ϕ -related distribution q . Representing q with θ -parametrized family of functions $h(\cdot|\theta)$, we may write $p(y|\phi, \epsilon)$ and $p(y|\phi)$ as

$$\begin{aligned} p(y|\phi) &\cong q_\theta(y|x) = h(y|x; \theta - \alpha \nabla_\theta \mathbb{E}[L_{\mathcal{E}}(\theta)]) & (7) \\ p(y|\phi, \epsilon) &\cong q_\theta(y|x, \epsilon) = h(y|x; \theta - \alpha \nabla_\theta L_\epsilon(\theta)). & (8) \end{aligned}$$

The advantage of this parametrization is multifold. First, when we evaluate these approximations empirically, the ϵ in our approximations only appears as an index in the empirical expectation. We do not have to use the *real* identity of ϵ in the evaluation of the approximation. Second, if the model is regular enough, we can expect $\mathbb{E}[q_\theta(y|x, \mathcal{E})] \cong q_\theta(y|x)$ for small enough α . Finally, by its design, $q_\theta(y|x, \epsilon)$ is closer to $p(y|x, \epsilon)$ than $q_\theta(y|x)$ at all time, agreeing with the requirement we stated above. See Appendix C.1 for more discussion about our parametrization. Now, $I(Y; \Phi)$ in (6) can be evaluated as $\mathbb{E}[L_{\mathcal{E}}(\theta)]$. The regularization term $I(Y; \mathcal{E}|\Phi)$ can be approximated as

$$\begin{aligned} I(Y; \mathcal{E}|\Phi) &\cong \mathbb{E}[d_{KL}(q_\theta(Y|X, \mathcal{E})||q_\theta(Y|X))] \\ &\cong \mathbb{E}[L_{\mathcal{E}}(\theta - \alpha \nabla_\theta \mathbb{E}[L_{\mathcal{E}}(\theta)]) - L_{\mathcal{E}}(\theta - \alpha \nabla_\theta L_{\mathcal{E}}(\theta))] \cong \alpha \text{trace}(\text{Var}(\nabla_\theta L_{\mathcal{E}}(\theta))). \end{aligned} \quad (9)$$

Thus, $q_\theta(y|x, \epsilon)$ is close to $q_\theta(y|x)$ if α is small. Figure 2 is an illustration of the relation of each ∇L_ϵ to the actual direction of update. For more detailed computation, see Appendix C.

4.2 Other OOD algorithms

IRM [1] is an algorithm that aims to achieve the same goal under the same set of assumptions. IRM practically assumes that, throughout the optimization process of both ϕ and the predictor function with respect to ϕ , the functional form of $\log p(y|\phi)$ is linear about ϕ . We, on the other hand, lift this condition at the price of becoming unable to explicitly identify the form of Φ in the predictor. IRM also does not derive its algorithm from a theoretically proven objective. Causal DAG based algorithms [29, 36] aims to identify the members of $Pa(Y)$ that maximizes the prediction performance. By its design, most of these algorithms require the user to use the knowledge of either the network itself or the DAG node-set. However, identification of causal DAG is itself a difficult problem that can require massive computation resources [7, 29], and it might not always be worth the effort if the sole purpose is to obtain the OOD-optimal inference model.

5 Experiment

We evaluated the efficacy of our method on *Colored-MNIST* and its extension. For more detail of the setting and the implementation, please see Appendix D.

5.1 Experimental setup

Extended Colored-MNIST (EC-MNIST) Because our extension generalizes the original *Colored-MNIST (C-MNIST)* in [1], we describe our *Extended Colored-MNIST (EC-MNIST)* first. Unlike the original C-MNIST, the invariant predictor set \mathcal{I} (3) in our version contains more than one variable. Our version is particularly different from the original one in that it can describe a case in which the domain invariant feature alone is not necessarily sufficient for the optimal environment-agnostic prediction. Each member of our EC-MNIST dataset is constructed as follows;

1. Set x_{ch2} to 1 with probability ϵ_{ch2} . Set it to 0 with probability $1 - \epsilon_{ch2}$.
2. Generate a binary label \hat{y}_{obs} from y with the following rule: $\hat{y}_{obs} = 0$ if $y \in \{0 \sim 4\}$ and $\hat{y}_{obs} = 1$ otherwise. If $\epsilon_{ch2} = k$, construct y_{obs} by flipping \hat{y}_{obs} with probability $p_k (k \in \{0, 1\})$.
3. Put $y_{obs} = \hat{x}_{ch0}$, and construct x_{ch0} from \hat{x}_{ch} by flipping \hat{x}_{ch1} with probability ϵ_{ch0} .
4. Construct x_{obs} as $x_{fig} \times [x_{ch0}, (1 - x_{ch0}), x_{ch2}]$. As an RGB image, this will come out as an image in which the red scale is *turned on* and the green scale is *turned off* if $x_{ch0} = 1$, and other-way around if $x_{ch0} = 0$. Blue scale is turned on only if $x_{ch2} = 1$.

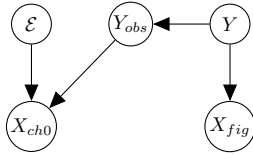


Figure 3: The graphical model of *C-MNIST*

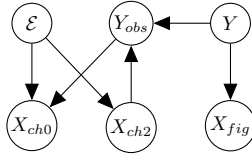
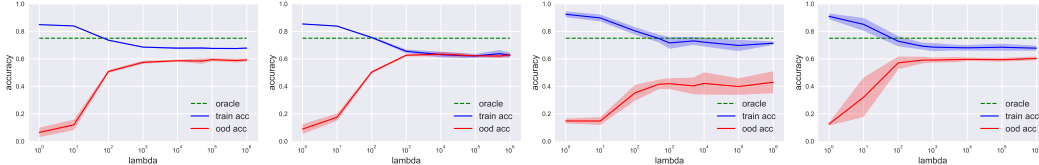


Figure 4: The graphical model of *EC-MNIST*

Model	OOD accuracy	
	<i>C-MNIST</i>	<i>EC-MNIST</i>
Oracle	0.75	0.75
X_{fig}	0.75	0.25
ERM	$0.172 \pm .029$	$0.176 \pm .029$
IRM	$0.592 \pm .011$	$0.430 \pm .080$
Ours	$0.620 \pm .015$	$0.594 \pm .013$

Table 3: Numerical performance of OOD algorithms. X_{fig} designates the *figure-only* oracle (i.e. the upper bound of ADA).



(a) IRM on *C-MNIST*

(b) Ours on *C-MNIST*

(c) IRM on *EC-MNIST*

(d) Ours on *EC-MNIST*

Figure 5: The plot of regularization parameter λ against the accuracies on *C-MNIST* ($p = 0.25$) and on *EC-MNIST* ($p_0 = 0.25, p_1 = 0.75$).

Figure 4 is the graphical model for the generation of *EC-MNIST*. In the experiment on this dataset, only (Y_{obs}, X_{obs}) are assumed observable. At training times, the machine learner will be given a set of datasets $\mathcal{D}_{train} = \{D_\epsilon; \epsilon \in R_{train}\}$ in which D_ϵ is a set of observations gathered when $\mathcal{E} = \epsilon$. In the test time, the learner will be challenged to make an inference of Y_{obs} from X_{obs} in the presence of an unknown environment ϵ^* . If ϵ^* is, far away from any members of R_{train} , overfitting of model to \mathcal{D}_{train} can result in catastrophic test performance.

For our *EC-MNIST*, Y_{obs} can be predicted at maximal probability of $\epsilon_{ch2} \max\{p_0, 1 - p_0\} + (1 - \epsilon_{ch2}) \max\{p_1, 1 - p_1\}$. In this problem, X_{fig} is a \mathcal{E} independent factor. At the same time, X_{ch2} is a member of \mathcal{I} , and X_{fig} together with X_{ch2} can create better predictor than X_{fig} alone. In fact, the oracle prediction by X_{fig} alone can attain an average value as high as $\max\{\epsilon_{ch2}p_0 + (1 - \epsilon_{ch2})p_1, \epsilon_{ch2}(1 - p_0) + (1 - \epsilon_{ch2})(1 - p_1)\}$, which is lower than the that of the $\{X_{fig}, X_{ch2}\}$ oracle. This follows from Fatou’s lemma [13]. In this problem, the oracle with X_{fig} alone coincides with the upper bound of Adversarial Domain Adaptation(ADA) [21]. Thus, ADA cannot provide an optimal solution in this case. IRM [1] also discusses such a case in their work.

Colored MNIST (C-MNIST): The original *C-MNIST* in [1] is a special case of our *EC-MNIST* in which the distribution of x_{ch2} does not vary with ϵ . Figure 3 is a schematic of the data generation process. Notice that if one uses X_{fig} alone, one can make the predictions at the optimal accuracy of $\max(1 - p, p)$. This is a situation that is considered in the study of ADA. In this sense, our *EC-MNIST* is more suited for the investigation of the pathological cases in OOD study.

5.2 Result

We compared our algorithm against Invariant Risk Minimization (IRM)[1], Empirical Risk Minimization (ERM), and the oracle(s).

Colored-MNIST The left column in table 3 compares the results of the algorithms in terms of the OOD accuracy (2). As we see in Table, our method outperforms both ERM and IRM. Figure 12(a)(b) plots the OOD accuracy against the regularization parameter. In general, larger regularization parameter promotes the OOD performance. The OOD accuracy plateaus around $\lambda \sim 10^4$.

Extended Colored-MNIST The right column in Table 3 compares the results of the algorithms in terms of the OOD performance (2). Again in this set of experiments, we perform better than ERM and IRM. We also perform better than the X_{fig} oracle. Because X_{ch2} is necessary in order to outperform the X_{fig} oracle (see section 5.1), our result suggests that we are actually using the feature X_{ch2} in making the prediction. Figure 12(c)(d) plots the OOD accuracy against the regularization parameter. Again, a larger regularization parameter generally promotes the OOD performance.

6 Relations to other topics

In an effort to address the problem similar to the OOD problem, the methods of *distributional robustness* [4, 16, 27, 32] use the notion of distance between a pair of distributions to bound the error between the loss over \mathcal{G}_{train} and the loss on the newly encountered environment. However, when one does not have much knowledge about the new distribution to encounter, it would be difficult to know the distance of the new distribution from the training set, let alone the appropriate metric to measure it. In our problem setting, we consider situations in which the distributional perturbation cannot be easily bounded numerically. In terms of application, *Fairness* is also a closely related field of study [26], and it aims to train a model whose output is invariant with respect to a particular environmental factor. However, it is essentially different from our study in that our study aims to train a model that works well a completely unknown environment.

Broader Impact

Our study is an effort toward the learning of a model that requires no additional dataset to perform well in a newly encountered environment. Further study in this field might allow safer/ more economical training of the model. For example, our study might allow the user to train a good model without collecting dataset from a dangerous/risky environment. Further study of the OOD problem might also be helpful in promoting the fairness of the prediction [26]. However, one must be wary of the treatment of the environmental factor. In this study, we consider the situations in which the identity of the environmental factor is unknown. This is actually the case in many applications; the effect of the hidden environmental factor might be observable only through the partition of datasets. In such cases, a user with ulterior motive might be able to fake the identity of the environment by using a particular partition of dataset. For example, when the mission is to train a model that can perform well on people of all ages, a user with ulterior motive might collect a dataset of one age group from a particular socio-political group and a dataset of another age group from a yet-another socio-political group. Such a user might advertise his/her predictor as an *age* agnostic predictor, when in truth the advertised environmental factor (*age*) do not agree with the true environmental factor. As it applies to many statistical methods, one must pay close attention to the data collection process in order to ensure the fair analysis.

References

- [1] Martin Arjovsky, Léon Bottou, Ishaan Gulrajani, and David Lopez-Paz. Invariant risk minimization. *arXiv preprint arXiv:1907.02893*, 2019.
- [2] Arindam Banerjee, Xin Guo, and Hui Wang. On the optimality of conditional expectation as a bregman predictor, 2003.
- [3] Shai Ben-David, John Blitzer, Koby Crammer, and Fernando Pereira. Analysis of representations for domain adaptation. In *Advances in neural information processing systems*, pages 137–144, 2007.
- [4] A. Ben-Tal, D. den Hertog, A.M.B. De Waegenaere, B. Melenberg, and G. Rennen. Robust solutions of optimization problems affected by uncertain probabilities. *Management Science*, 59(2):341–357, 2013. Appeared earlier as CentER Discussion Paper 2011-061.
- [5] Yoshua Bengio, Tristan Deleu, Nasim Rahaman, Nan Rosemary Ke, Sebastien Lachapelle, Olexa Bilaniuk, Anirudh Goyal, and Christopher Pal. A meta-transfer objective for learning to disentangle causal mechanisms. In *International Conference on Learning Representations*, 2020.
- [6] Christopher M. Bishop. *Pattern Recognition and Machine Learning (Information Science and Statistics)*. 2007.
- [7] Peter Bühlmann. Invariance, causality and robustness. *arXiv preprint arXiv:1812.08233*, 2018.
- [8] Enrique Castillo, Jose M Gutierrez, and Ali S Hadi. *Expert systems and probabilistic network models*. Springer Science & Business Media, 2012.

- [9] Djork-Arné Clevert, Thomas Unterthiner, and Sepp Hochreiter. Fast and accurate deep network learning by exponential linear units (elus). *arXiv preprint arXiv:1511.07289*, 2015.
- [10] G. Darmais. Analyse gnrale des liaisons stochastiques: etude particulire de l’analyse factorielle linnaire. *Revue de l’Institut International de Statistique / Review of the International Statistical Institute*, 21(1/2):2–8, 1953.
- [11] Rick Durrett. *Probability: Theory and Examples*. Thomson, 2019.
- [12] Huszár Ferenc. Invariant risk minimization: An information theoretic view. 2019.
- [13] Gerald B Folland. *Real analysis: modern techniques and their applications*. John Wiley & Sons, 2013.
- [14] Maxime Gasse. *Probabilistic Graphical Model Structure Learning: Application to Multi-Label Classification*. PhD thesis, 2017.
- [15] Robert Geirhos, Patricia Rubisch, Claudio Michaelis, Matthias Bethge, Felix A. Wichmann, and Wieland Brendel. Imagenet-trained CNNs are biased towards texture; increasing shape bias improves accuracy and robustness. In *International Conference on Learning Representations*, 2019.
- [16] Weihua Hu, Gang Niu, Issei Sato, and Masashi Sugiyama. Does distributionally robust supervised learning give robust classifiers? In Jennifer Dy and Andreas Krause, editors, *Proceedings of the 35th International Conference on Machine Learning*, volume 80 of *Proceedings of Machine Learning Research*, pages 2029–2037, Stockholmsmssan, Stockholm Sweden, 10–15 Jul 2018. PMLR.
- [17] Andrew Ilyas, Shibani Santurkar, Dimitris Tsipras, Logan Engstrom, Brandon Tran, and Aleksander Madry. Adversarial examples are not bugs, they are features. In H. Wallach, H. Larochelle, A. Beygelzimer, F. d Alché-Buc, E. Fox, and R. Garnett, editors, *Advances in Neural Information Processing Systems 32*, pages 125–136. Curran Associates, Inc., 2019.
- [18] Sergey Ioffe and Christian Szegedy. Batch normalization: Accelerating deep network training by reducing internal covariate shift. *arXiv preprint arXiv:1502.03167*, 2015.
- [19] Fredrik D. Johansson, David Sontag, and Rajesh Ranganath. Support and invertibility in domain-invariant representations. In Kamalika Chaudhuri and Masashi Sugiyama, editors, *Proceedings of Machine Learning Research*, volume 89 of *Proceedings of Machine Learning Research*, pages 527–536. PMLR, 16–18 Apr 2019.
- [20] Diederik P Kingma and Jimmy Ba. Adam: A method for stochastic optimization. *arXiv preprint arXiv:1412.6980*, 2014.
- [21] Haoliang Li, Sinno Jialin Pan, Shiqi Wang, and Alex C Kot. Domain generalization with adversarial feature learning. In *Proceedings of the IEEE Conference on Computer Vision and Pattern Recognition*, pages 5400–5409, 2018.
- [22] Ya Li, Mingming Gong, Xinmei Tian, Tongliang Liu, and Dacheng Tao. Domain generalization via conditional invariant representations. In *Thirty-Second AAAI Conference on Artificial Intelligence*, 2018.
- [23] Ya Li, Xinmei Tian, Mingming Gong, Yajing Liu, Tongliang Liu, Kun Zhang, and Dacheng Tao. Deep domain generalization via conditional invariant adversarial networks. In *Proceedings of the European Conference on Computer Vision (ECCV)*, pages 624–639, 2018.
- [24] Peter Lucas, José A Gámez, and Antonio Salmerón Cerdan. *Advances in Probabilistic Graphical Models*, volume 213. Springer, 2007.
- [25] Sara Magliacane, Thijs van Ommen, Tom Claassen, Stephan Bongers, Philip Versteeg, and Joris M Mooij. Domain adaptation by using causal inference to predict invariant conditional distributions. In *Advances in Neural Information Processing Systems*, pages 10846–10856, 2018.

- [26] Ninareh Mehrabi, Fred Morstatter, Nripsuta Saxena, Kristina Lerman, and Aram Galstyan. A survey on bias and fairness in machine learning. *arXiv preprint arXiv:1908.09635*, 2019.
- [27] Amir Najafi, Shin-ichi Maeda, Masanori Koyama, and Takeru Miyato. Robustness to adversarial perturbations in learning from incomplete data. In *Advances in Neural Information Processing Systems 32*, pages 5542–5552. Curran Associates, Inc., 2019.
- [28] Judea Pearl et al. Causal inference in statistics: An overview. *Statistics surveys*, 3:96–146, 2009.
- [29] J. Peters, P. Bühlmann, and N. Meinshausen. Causal inference using invariant prediction: identification and confidence intervals. *Journal of the Royal Statistical Society, Series B (with discussion)*, 78(5):947–1012, 2016.
- [30] Mateo Rojas-Carulla, Bernhard Schölkopf, Richard Turner, and Jonas Peters. Invariant models for causal transfer learning. *The Journal of Machine Learning Research*, 19(1):1309–1342, 2018.
- [31] Dominik Rothenhäusler, Nicolai Meinshausen, Peter Bühlmann, and Jonas Peters. Anchor regression: heterogeneous data meets causality. *arXiv preprint arXiv:1801.06229*, 2018.
- [32] Soroosh Shafieezadeh Abadeh, Peyman Mohajerin Mohajerin Esfahani, and Daniel Kuhn. Distributionally robust logistic regression. In C. Cortes, N. D. Lawrence, D. D. Lee, M. Sugiyama, and R. Garnett, editors, *Advances in Neural Information Processing Systems 28*, pages 1576–1584. Curran Associates, Inc., 2015.
- [33] Zheyuan Shen, Peng Cui, Kun Kuang, Bo Li, and Peixuan Chen. Causally regularized learning with agnostic data selection bias. In *Proceedings of the 26th ACM international conference on Multimedia*, pages 411–419, 2018.
- [34] Hidetoshi Shimodaira. Improving predictive inference under covariate shift by weighting the log-likelihood function. *Journal of Statistical Planning and Inference*, 90(2):227–244, October 2000.
- [35] Amos Storkey. When training and test sets are different: characterizing learning transfer. *Dataset shift in machine learning*, pages 3–28, 2009.
- [36] Adarsh Subbaswamy, Peter Schulam, and Suchi Saria. Preventing failures due to dataset shift: Learning predictive models that transport. In Kamalika Chaudhuri and Masashi Sugiyama, editors, *Proceedings of Machine Learning Research*, volume 89 of *Proceedings of Machine Learning Research*, pages 3118–3127. PMLR, 16–18 Apr 2019.
- [37] Yexun Zhang, Ya Zhang, Yanfeng Wang, and Qi Tian. Domain-invariant adversarial learning for unsupervised domain adaptation. *arXiv preprint arXiv:1811.12751*, 2018.
- [38] Han Zhao, Remi Tachet des Combes, Kun Zhang, and Geoffrey J Gordon. On learning invariant representation for domain adaptation. *arXiv preprint arXiv:1901.09453*, 2019.

Appendix

A Why invariant features?

We give more explanation about our motivation in solving the OOD problem. As mentioned in the introduction, OOD problem arises when one has to deal with sets of datasets coming from possibly different distributions. For example, when we are to conduct image-recognition from a dataset of animal pictures collected by a group of photographers, we might have to consider the fact that some photographer might favor a picture of a given animal in a certain posture at a certain set of locations at a certain time of the day, and some do not. If *camel* happens to be always found in desert in the set of pictures taken by *Jerry* the photographer, an *animal classifier* trained on his dataset may characterize *camel* as *a horse-like figure in desert*. Meanwhile, it might be the case that *Tom* the photographer prefers to take a picture of any animal at a zoo. Indeed, the *animal classifier* trained on *Jerry*'s dataset will most likely fail to recognize *Tom*'s picture of camel as *camel*, because a picture of a *camel in a cage* does not agree with the *description of the camel* learned by the classifier.

Such behavior shall not be considered as a *bug*, because *a horse-like figure in desert* is definitely a characterizing description of *camel* on the distribution that underlies the set of natural images taken by *Jerry*. This type of problem can arise in a more subtle way. Some studies report that in practice, the machine learner may associate the label with even more subtle features like a texture or a pixel-pattern that cannot be discerned by humans [17, 15].

Then how shall we formalize what is "reasonable" and what is not? If the system of concern is governed by a certain causal relation, the exterior factor can only affect the input-output distribution in a certain way, and some parts of the relations in the system will remain unchanged [28, 7]. We can borrow from this philosophy; we can say that the exterior factor is affecting the distribution in a "reasonable" manner if there is always some part of the input-output relation that remains invariant under its influence. We can then work with the assumption that some part of the input-output relation is shared in common by all distributions to be considered. For the aforementioned *camel* example, camels' *essential biological feature* in the picture is not affected by the person who takes the picture. This is an example of the approach based on invariance. By finding the part of the system that stays invariant under the effect of environmental factor, one may be able to find a solution to the OOD problem. Our study explains when this is actually possible.

We do not necessarily say that this is the only way to go in all situations. For example, if environmental factor and its effects are known in advance, we may take a completely different strategy. In the animal picture recognition problem we mentioned above, if we know from the beginning that "photographer" is the environmental factor and that they affect the "background" part of the image, one may be able to improve the generalization ability of the trained model by allowing it to leverage the similarity relations among the photographers. In such cases, methods of distributional robustness might be particularly helpful [4, 16, 27, 32].

But in many cases, figuring out what is affecting the dataset is a difficult problem on its own, and it is often not known how similar the new photographer is to the set of photographers we have seen. This is the motivation behind the invariance-based approach to the OOD problem.

B Proof of the Invariance Results

In this section we provide the proofs for the theoretical results we presented in the section 3 of the main manuscript. Let \mathcal{E} , X , Y be random variables defined with probability triple (Ω, \mathcal{F}, P) . Throughout, we will follow the notation rules we introduced in the main part of the manuscript. Following the convention in probability, we use $\sigma(Z)$ to denote a sigma algebra generated by X , and write $W \in \sigma(Z)$ whenever W is measurable with respect to Z . We will generally use upper case letters to denote random variables, and use lower case letters to denote the corresponding realizations. Unless otherwise noted, we will use \mathbb{E} to represent the expectation with respect to P . We will also use \perp to represent independency relation, and use $A \perp B|C$ to convey that $P(A, B|C) = P(A|C)P(B|C)$.

Now, let Φ be a random variable that is measurable with respect to $\sigma(X)$, and let us define the following elements that can be derived from Φ :

1. $\mathcal{F}_\psi = \{E \in \sigma(\mathcal{E}); E \perp \Phi\}$ is a set of random variables representable as a function of \mathcal{E} that are independent from variable Φ
2. $\mathcal{E}_\psi \in \mathcal{F}_\psi$. If it exists, we define this to be a random variable that is maximal in the sense that there is no other $Z \in \mathcal{F}_\psi$ with $\sigma(\mathcal{E}_\psi) \subsetneq \sigma(Z)$.
3. $\mathcal{E}_\phi = \mathcal{E}_\psi^c$; that is, $\mathcal{E}_\phi \perp \mathcal{E}_\psi$ and $\sigma(\mathcal{E}_\phi, \mathcal{E}_\psi) = \sigma(\mathcal{E})$.

As for the existence of the last decomposition, we appeal to the result of [10], which claims that, for any joint distribution of (X, Y) we can find a function f and a noise $N_Y \perp X$, such that $Y = f(X, N_Y)$. Therefore, for every $\epsilon \in \text{supp}(\mathcal{E})$, let us WLOG suppose a map r for which $r(\epsilon_\phi, \epsilon_\psi) = \epsilon$, and use $(\epsilon_\phi, \epsilon_\psi)$ and ϵ interchangeably. Let us also define the invariant set \mathcal{I} by

$$\mathcal{I} = \{\Phi \in \sigma(X); (Y|\Phi, \mathcal{E}) = (Y|\Phi), Y \not\perp \Phi\} \quad (10)$$

and that this set is non-empty. Then the following lemma will be useful for the main result B.2, which provides a set of conditions under which the $\Phi \in \mathcal{I}$ satisfies the OOD optimality:

Lemma B.1. *If $\Phi \in \mathcal{I}$, then $\mathcal{E}_\psi \perp (\Phi, Y)$.*

Proof. By definition, $Y \perp \mathcal{E}|\Phi$ so in particular, $Y \perp \mathcal{E}_\psi|\Phi$ and $Y \perp \mathcal{E}_\phi|\Phi$. Moreover, by definition, $\mathcal{E}_\psi \perp \Phi$. Thus $P(\mathcal{E}_\psi|Y, \Phi) = P(\mathcal{E}_\psi|\Phi) = P(\mathcal{E}_\psi)$ and $\mathcal{E}_\psi \perp (\Phi, Y)$, as desired. \square

We are now ready to present the proposition B.2. In an equation that uses multiple \mathbb{E} notation, will use a notation like \mathbb{E}_Z to help seeing that the inside the symbol is an integration about Z .

Proposition B.2. *Let g be a strictly convex, differentiable function and let D be the corresponding Bregman Loss function. Let $\Phi \in \sigma(\mathcal{I})$, and let w_ϕ be the measurable function such that $\Phi = w_\phi(X)$. Also, put $f^*(X) = \mathbb{E}[Y|\Phi] = g^*(w_\phi(X))$ and suppose that, for all ϵ_ϕ there exists $\tilde{\epsilon}_\psi$ such that*

$$X \perp Y | (\Phi, \epsilon_\phi, \tilde{\epsilon}_\psi) \quad (11)$$

Then

$$f^* = \arg \min_f \sup_{\epsilon \in \text{supp}(\mathcal{E})} \mathbb{E}[D(f(X), Y)|\epsilon] \quad (12)$$

Proof. We are going to leverage the fact that, if \mathcal{G} is a sub sigma algebra of \mathcal{F} to which Y is measurable, then [2]

$$\arg \min_{Z \in \mathcal{G}} \mathbb{E}[D(Z, Y)] = \mathbb{E}[Y|\mathcal{G}]. \quad (13)$$

We are also going to use the fact that the Bregman loss function

$$D(a, b) = g(a) - g(b) - \langle a - b, \nabla g(b) \rangle$$

is convex about its first coordinate, a . Now, in order to show the claim, we need to show that $\sup_\epsilon \mathbb{E}[D(f(X), Y)|\epsilon] \geq \sup_\epsilon \mathbb{E}[D(f^*(X), Y)|\epsilon]$ for all measurable f . To show this, for any fixed ϵ we need to be able to find one ϵ' such that

$$\mathbb{E}[D(f(X), Y)|\epsilon'] \geq \mathbb{E}[(D(f^*(X), Y)|\epsilon)]. \quad (14)$$

Suppose a fixed ϵ and suppose that $\epsilon = r(\epsilon_\phi, \epsilon_\psi)$ for the appropriate invertible map r , and let ϵ' be such that $\epsilon' = r(\epsilon_\phi, \tilde{\epsilon}_\psi)$ with $\tilde{\epsilon}_\psi$ that satisfies the condition in the claim. Now, the Bregman Loss function $D(x, y)$ is convex with respect to x . With Jensen's inequality and repeated application of Tower rule [11],

$$\mathbb{E}_{X, Y}[D(f(X), Y)|\epsilon'] = \mathbb{E}_{\Phi, Y}[\mathbb{E}_X[D(f(X), Y)|\epsilon', \Phi, Y]] \quad (15)$$

$$\geq \mathbb{E}_{\Phi, Y}[D(\mathbb{E}_X[f(X)|\Phi, Y, \epsilon'], Y)|\epsilon'] \quad (16)$$

$$= \mathbb{E}_{\Phi, Y}[(D(\mathbb{E}_X[f(X)|\Phi, \epsilon'], Y)|\epsilon')] \quad (17)$$

$$= \mathbb{E}_{\Phi, Y}[D(h(\Phi, \epsilon'), Y)|\epsilon'] \quad (18)$$

where we set $h(\Phi, \epsilon') = \mathbb{E}[f(X)|\Phi, \epsilon']$ and used Jensen's inequality in the second line. Here, the random variable that is integrated in the last expression is Φ and Y only, and $\epsilon_\phi, \epsilon_\psi, \tilde{\epsilon}_\psi$ are all

constant. Moreover, by the lemma B.1, $(Y, \Phi)|_{\epsilon_\phi, \tilde{\epsilon}_\psi} = (Y, \Phi)|_{\epsilon_\phi, \epsilon_\psi}$. Therefore, using the property of $\tilde{\epsilon}_\psi$,

$$\mathbb{E}_{\Phi, Y}[D(h(\Phi, \epsilon'), Y)|_{\epsilon_\phi, \tilde{\epsilon}_\psi}] = \mathbb{E}_{\Phi, Y}[D(h(\Phi, \epsilon_\phi, \tilde{\epsilon}_\psi), Y)|_{\epsilon_\phi, \tilde{\epsilon}_\psi}] \quad (19)$$

$$= \mathbb{E}_{\Phi, Y}[D(h(\Phi, \epsilon_\phi, \tilde{\epsilon}_\psi), Y)|_{\epsilon_\phi, \epsilon_\psi}] \quad (20)$$

$$\geq \mathbb{E}_{\Phi, Y}[D(\mathbb{E}_Y[Y|\Phi, \epsilon_\phi, \epsilon_\psi], Y)|_{\epsilon_\phi, \epsilon_\psi}] \quad (21)$$

$$= \mathbb{E}_{\Phi, Y}[D(\mathbb{E}[Y|\Phi], Y)|_{\epsilon_\phi, \epsilon_\psi}] \quad (22)$$

$$= \mathbb{E}_{\Phi, Y}[D(f^*(X), Y)|_{\epsilon_\phi, \epsilon_\psi}] \quad (23)$$

Above, the inequality in the third line follows just from the optimality of the conditional expectation about the Bregman divergence, and the equality in the fourth line follows from the fact that $\Phi \in \mathcal{I}$.

All together we have

$$\mathbb{E}[D(f(X), Y)|_{\epsilon'}] \geq [D(f^*(X), Y)|_{\epsilon}]. \quad (24)$$

□

Indeed, the condition in the claim B.2 does not hold for just any arbitrary $\Phi \in \mathcal{I}$. In order for $g^*(\Phi)$ to be optimal in the sense of B.2, Φ has to be special in some sense.

Proposition B.3. *Suppose $\Phi \in \mathcal{I}$ and suppose that ϵ satisfies $X \perp Y|\Phi, \epsilon$. Then for this particular ϵ ,*

$$\Phi = \arg \max_{Z \in \sigma(X)} I(Y; Z|\epsilon).$$

Proof. Suppose that there exists $B \in \sigma(X)$ with $I(Y; B, \Phi|\epsilon) > I(Y; \Phi|\epsilon)$. Notice then that

$$I(Y; B, \Phi|\epsilon) = I(Y; \Phi|\epsilon) + I(Y; B|\Phi, \epsilon) \quad (25)$$

and it follows that $I(Y; B|\Phi, \epsilon) > 0$. Since $I(Y; X|\Phi, \epsilon) \geq I(Y; B|\Phi, \epsilon)$ this implies that $Y \not\perp X|\Phi, \epsilon$ and in particular, ϵ does not satisfy $X \perp Y|\Phi, \epsilon$. Thus, in order for $X \perp Y|\Phi, \epsilon$ to hold for ϵ , such B cannot exist. In other words, Φ must be optimal among all $Z \in \sigma(X)$ on any environment satisfying (11). □

The necessary condition for (11) can be also more succinctly stated as follows.

Proposition B.4. *Suppose $\Phi \in \mathcal{I}$ and suppose that for some ϵ^* , $\Phi \perp Y|\epsilon^*$. Then there exists no $\tilde{\Phi} \in \mathcal{I}$ with $\tilde{\Phi} \in \sigma(\tilde{\Phi})$ such that $I(Y; \tilde{\Phi}) < I(Y; \Phi)$.*

Proof. Let $\tilde{\Phi}$ be as stated in the assumption. Then since $g(X) \perp Y|\Phi, \epsilon^*$, it particularly follows that $\tilde{\Phi}(X) \perp Y|\epsilon^*$. Thus we have

$$P(Y|\tilde{\Phi}) = P(Y|\tilde{\Phi}, \epsilon^*) \quad (26)$$

$$= P(Y|\tilde{\Phi}, \Phi, \epsilon^*) \quad (27)$$

$$= P(Y|\Phi, \epsilon^*) \quad (28)$$

$$= P(Y|\Phi) \quad (29)$$

Where the first and the last equalities follow from the invariance property, the second equality follows from the tower rule of conditional expectation, and the third equality follows from the assumption about ϵ^* . Note that both Φ and $\tilde{\Phi}$ are functions about X . Also, note that the mutual information depends only on conditional distribution. It follows that $I(Y; \tilde{\Phi}) = I(Y; \Phi)$, and the claim follows. □

Theorem B.5. *Suppose that there exists at least one Φ for which there is a corresponding ϵ_ψ for every ϵ_ϕ such that $X \perp Y|\Phi, \epsilon_\phi, \epsilon_\psi$. Suppose also that \mathcal{I} is generated by one Φ_0 . In this case $E[Y|\Phi^*]$ is OOD optimal if*

$$\Phi^* = \arg \max_{\Phi \in \mathcal{I}} I(Y; \Phi). \quad (30)$$

Proof. If $\tilde{\Phi} \in \mathcal{I}$ is such that for every ϵ_ϕ there is a corresponding ϵ_ψ , $\tilde{\Phi}$ is automatically OOD optimal, and it needs to be maximal by the proposition B.4. Now, if \mathcal{I} is generated by one Φ_0 , then Φ_0 is the unique maximal variable in the sense that it is equivalent to Φ^* up to its sigma field. Because $\tilde{\Phi} \in \sigma(\Phi_0)$, $\sigma(\Phi_0) = \sigma(\tilde{\Phi})$ necessarily by the maximality of $\tilde{\Phi}$ as well. We thus have $\sigma(\Phi_0) = \sigma(\tilde{\Phi}) = \sigma(\Phi^*)$. Thus, for Φ_0 there exists ϵ_ψ satisfying 11 for every ϵ_ϕ , and $E[Y|\Phi_0] = E[Y|\Phi^*]$ is OOD optimal. \square

As one *explicit* example, that \mathcal{I} is generated by one variable can happen when the underlying distribution P is UG-faithful, that is, P is faithful to the independence relations for which there exists some undirected graph G that induces a perfect map [14, 24, 8] More succinctly stated, we have the following corollary.

Corollary B.6. *Suppose that there exists at least one Φ for which there is a corresponding ϵ_ψ for every ϵ_ϕ such that $X \perp Y|\Phi, \epsilon_\phi, \epsilon_\psi$, and suppose that P is UG-faithful to some undirected graph. Then MIP implies OOD optimality.*

Proof. If P is UG-faithful to some undirected graph, we know that strong union law of the conditional independence applies. That is, if $X \perp Y|\Phi_1, \mathcal{E}$ and $X \perp Y|\Phi_2, \mathcal{E}$, then $X \perp Y|\Phi_1, \Phi_2, \mathcal{E}$ as well. Let Φ^* be a MIP. If there exists another $\tilde{\Phi} \in \mathcal{I}$ such that $\tilde{\Phi} \notin \sigma(\Phi^*)$, then $\Phi_0 = [\tilde{\Phi}, \Phi^*]$ has larger mutual information than Φ^* . Also, by the strong union property, $\Phi_0 \in \mathcal{I}$. This contradicts the maximality of Φ^* , so $\mathcal{I} = \sigma(\Phi^*)$ necessarily, and the claim follows by the application of the theorem B. \square

This corollary might be applicable to some DAG cases as well. For more detailed relation between DAG and undirected graph, see [6]. We shall also mention that, when P is UG-faithful to some undirected graph, the MIP is everything that excludes \mathcal{E} and Y . As we emphasize over and over, we are considering the case in which the identity of \mathcal{E} as well as the correlation amongst the covariates and variates, so even if it is known that P is faithful to *some* undirected graph, finding MIP might be better strategy in such case.

The following is another sufficient condition for the OOD optimality that can hold if we can make a slightly stronger assumption about \mathcal{E} .

Corollary B.7. *Suppose that \mathcal{E} admits an independence decomposition $(\mathcal{E}_\phi, \mathcal{E}_\psi)$ such that $\mathcal{E}_\psi = \mathcal{E}_\phi^c$ and $\mathcal{E}_\phi \perp \Psi$. If there exists one $\tilde{\epsilon}_\psi$ for which $\Psi \perp Y|\tilde{\epsilon}_\psi$, then $\mathbb{E}[Y|\Phi]$ is OOD optimal.*

Proof. Since $\Phi \perp (\Psi, \mathcal{E}_\psi)$, we have $(\Phi \perp \Psi)|\mathcal{E}_\psi$ because

$$P(\Phi|\Psi, \mathcal{E}_\psi) = P(\Phi) = P(\Phi|\mathcal{E}_\psi) \quad (31)$$

Likewise, by the assumption we have $\mathcal{E}_\phi \perp (\Psi, \mathcal{E}_\psi)$, so we have $(\mathcal{E}_\phi \perp \Psi)|\mathcal{E}_\psi$. Now, we also have the assumption that $\Psi \perp Y|\tilde{\epsilon}_\psi$. Altogether we have $(\Psi \perp (Y, \mathcal{E}_\phi, \Phi))|\tilde{\epsilon}_\psi$. This tells us that

$$P(\Psi|Y, \mathcal{E}_\phi, \Phi, \tilde{\epsilon}_\psi) = P(\Psi|\tilde{\epsilon}_\psi) = P(\Psi|Y, \tilde{\epsilon}_\psi) \quad (32)$$

This is to say that $\Psi \perp Y|\Phi, \mathcal{E}_\phi, \tilde{\epsilon}_\psi$, and the claim follows by the application of B.2. \square

We also want to make a comment regarding the choice of \mathcal{E}_ψ .

Remark B.8. *Making \mathcal{E}_ψ maximal in the assumption 3 in general cases the difficulty of satisfying 11. To see this, suppose that \mathcal{E}_ψ is not maximal, and that there exists $\tilde{\mathcal{E}}_\psi$ with the corresponding complement $\tilde{\mathcal{E}}_\phi$ for which $\sigma(\tilde{\mathcal{E}}_\psi) \subsetneq \mathcal{E}_\psi$. Now, again in the way of [10], let $\mathcal{E}'_\psi \perp \mathcal{E}_\psi$ be such that $\sigma(\mathcal{E}'_\psi, \mathcal{E}_\psi) = \sigma(\tilde{\mathcal{E}}_\psi)$. This way we can let the triplet $(\tilde{\mathcal{E}}_\phi, \mathcal{E}'_\psi, \mathcal{E}_\psi)$ to represent e , and let the pair $(\tilde{\mathcal{E}}_\phi, \mathcal{E}'_\psi)$ serve as a \mathcal{E}_ϕ . Whenever one can say that, for all ϵ_ϕ there exists ϵ_ψ satisfying (11), I can also say as well that, for all $\tilde{\epsilon}_\phi$ there exists $\tilde{\epsilon}_\psi = (\epsilon'_\psi, \epsilon_\psi)$ for which (11) holds. This is clear by construction. However, the reverse is not true in general. Even if for $\tilde{\epsilon}_\phi$ there exists $\tilde{\epsilon}_\psi$ for which (11) holds, it is not necessarily true that, for all ϵ_ϕ there exists ϵ_ψ satisfying (11). To see this, suppose that, for a given $\tilde{\epsilon}_\phi$, there is a unique $(\epsilon'^*_\psi, \epsilon^*_\psi)$ such that (11) holds. In this case, for any $\epsilon_\phi = (\tilde{\epsilon}_\phi, \epsilon'_\psi)$ with $\epsilon'_\psi \neq \epsilon'^*_\psi$, there is no ϵ_ψ for which (11) holds.*



Figure 6: (Left) A rough schematic view of the condition assumed in the corollary B.7, interpreted in the language of graphical model. (Right) When there is a $\tilde{\epsilon}_\psi$ that breaks the edge from Y to Ψ , the conditional expectation $\mathbb{E}[Y|\Phi]$ will be OOD optimal.

C More details about Method

C.1 Difficulties in finding the MIP

At a first glance, the concept we presented in the last section seems to require two steps: (i) the search for the solution Φ^* of (30) and (ii) the computation of $\mathbb{E}[Y|\Phi^*]$, which is a function of Φ^* . However, finding Φ^* is difficult on its own because $I(Y; \Phi)$ requires $p(Y|\Phi)$ (density) for its evaluation. Without reasonably accurate knowledge about the density of X and Y , it is hard to compute (30), let alone the condition for Φ 's invariance.

Classic constrained optimization methods often use regularization terms to enforce the constraint. Let us use Q to approximate P , and let us parametrize Q by ξ and Φ by η . We can interpret our problem (30) as the optimization of

$$\begin{aligned} \arg \min_{\xi, \eta} \mathbb{E}[d_{KL}[p(Y|X)||p(Y|\Phi_\eta)]] \\ + \mathbb{E}[d_{KL}[p(Y|\Phi_\eta)||q_\xi(Y|\Phi_\eta)]] + \lambda I_q(Y; \mathcal{E}|\Phi_\eta) \end{aligned} \quad (33)$$

about both Φ and q . The last regularization term encourages Φ to be in \mathcal{I} , and the second term encourages q to be close to p . The first term encourages Φ to be closely correlated with Y . Now, $I_q(Y, \mathcal{E}|\Phi_\eta)$ can be approximated by

$$\mathbb{E}[d_{KL}(q_\xi(Y|\Phi_\eta, \mathcal{E})||q_\xi(Y|\Phi_\eta))] \quad (34)$$

and it also follows that

$$\begin{aligned} \mathbb{E}[d_{KL}[p(Y|X)||q_\xi(Y|\Phi_\eta)]] \\ = \mathbb{E}[d_{KL}[p(Y|X)||p(Y|\Phi_\eta)]] \\ + \mathbb{E}[d_{KL}[p(Y|\Phi_\eta)||q_\xi(Y|\Phi_\eta)]]. \end{aligned} \quad (35)$$

With the understanding that the pair of the parameters (ξ, η) represents a function, let us write $d_{KL}[p(Y|X)||q_\xi(Y|\Phi_\eta)]$ as $L_e(\xi, \eta)$. We can think of (33) as the minimizer of the following equation about ξ, η ;

$$\mathbb{E}[L_e(\xi, \eta)] + \lambda \mathbb{E}[d_{KL}(q_\xi(Y|\Phi_\eta, \mathcal{E})||q_\xi(Y|\Phi_\eta))]. \quad (36)$$

However, we encounter another problem yet again. In general, the form of $q(y|\phi)$ as a function of ϕ depends on the choice of ϕ ⁵. This problem is subtle but important. For instance, if $q_\xi(y|\phi_\eta)$ is modeled as $f(y, x, \xi, \eta)$, then $f(y, x, \xi, \eta')$ for $\eta' \neq \eta$ is generally not equal to $q_\xi(y|\phi_{\eta'})$. Rather, it will most likely equal $\tilde{q}_\xi(y|\phi_{\eta'})$ for completely other \tilde{q}_ξ . To see this, note that $q_\xi(y|\phi_{\eta'})$ is solution about the optimization of $\arg \min_r d_{KL}[q_\xi(y|\phi_\eta)||r(y|\phi_{\eta'})]$ about the density r , and it is clear that the optimal r depends on η . Thus, the choice of η and the choice of ξ are not independent, and the simultaneous update of ξ and η can be nonsensical.

While aiming for different invariant feature, IRM[1] too encountered a similar problem and endeavored to skirt this problem by assuming that $\mathbb{E}[Y|\Phi]$ is linear with respect to Φ , and modeled $\mathbb{E}[Y|\Phi] = \langle \mathbf{1}, \Phi \rangle$ by requiring Φ to absorb all linear transformation. However, it is unlikely that $\mathbb{E}[Y|\Phi]$ takes the same form throughout the algorithm in search of a good Φ . The same things can be said to $P(Y \in A|\Phi)$ for any A , which is, in essence, $\mathbb{E}[1_A(Y)|Z]$.

⁵Recall that ϕ is a symbol representing the realization of Φ

C.2 Penalty derivation

In this section, we provide the derivation of the penalty term we omitted in the section 4.2. For the notations, please take a look at the main manuscript.

$$I(Y; \mathcal{E} | \Phi) \cong I_q(Y; \mathcal{E} | \Phi) = \mathbb{E}[d_{KL}(q_\theta(Y|X, \mathcal{E}) || q_\theta(Y|X))] \quad (37)$$

$$\cong \mathbb{E}[\log q_\theta(Y|X, \mathcal{E}) - \log q_\theta(Y|X)] \quad (38)$$

$$= \mathbb{E}[L_{\mathcal{E}}(\theta - \alpha \nabla_\theta \mathbb{E}[L_{\mathcal{E}}(\theta)]) - L_{\mathcal{E}}(\theta - \alpha \nabla_\theta L_{\mathcal{E}}(\theta))] \quad (39)$$

$$\cong \alpha (\mathbb{E}[\nabla_\theta L_{\mathcal{E}}(\theta)^T \nabla_\theta L_{\mathcal{E}}(\theta)] - \mathbb{E}[\nabla_\theta L_{\mathcal{E}}(\theta)]^T \mathbb{E}[\nabla_\theta L_{\mathcal{E}}(\theta)]) \quad (40)$$

$$= \alpha \text{trace}(\text{Var}(\nabla_\theta L_{\mathcal{E}}(\theta))) \quad (41)$$

Also, in our implementation, we took advantage of the smallness of α to approximate $q(y|x; \theta)$ in the first term with $g(y|x; \theta)$ instead of $g(y|x; \theta - \alpha \nabla_\theta \mathbb{E}[L_e(\theta)])$. In fact, faithfully computing the first term with $g(y|x; \theta - \alpha \nabla_\theta \mathbb{E}[L_{\mathcal{E}}(\theta)])$ did not make much difference in the training process.

D Implementation Detail

In this section we describe the details of the experiment design along with the architectures of the models we used. In order to present a self-contained material, we first restate the experimental setting we already described in the main manuscript.

D.1 Colored MNIST

Colored MNIST is an experiment that was used in [1]. The goal of the task in *Colored MNIST* is to predict the label of a given digit in the presence of varying exterior factor, \mathcal{E} . The left panel of the figure 8 is a Bayesian Network representation of this experiment. Each member of the *Colored MNIST* dataset is constructed from an image-label pair (x, y) in MNIST, as follows.

1. Assign a binary label \hat{y}_{obs} from y with the following rule: $\hat{y}_{obs} = 0$ if $y \in \{0 \sim 4\}$ and $\hat{y}_{obs} = 1$ otherwise.
2. Flip \hat{y}_{obs} with a fixed probability p to produce y_{obs} .
3. Let x_{fig} be the binary image corresponding to y .
4. Put $y_{obs} = \hat{x}_{ch1}$, and construct x_{ch1} from \hat{x}_{ch1} by flipping \hat{x}_{ch1} with probability e .
5. Construct $x_{ods} = x_{fig} \times [x_{ch0}, (1 - x_{ch0}), 0]$. (that is, red if $x_{ch1} = 1$ and green if $x_{ch1} = 0$.)
Indeed, x_{obs} has exactly same information as the pair (x_{fig}, x_{ch1}) .

In this experiment, only (Y_{obs}, X_{obs}) are assumed observable. At training times, the machine learner will be given a set of datasets $\mathcal{D}_{train} = \{D_e; e \in R_{train}\}$ in which D_e is a set of observations gathered when $\mathcal{E} = e$. We set $|R_{train}| = 2$, and choose $|D_e| = 25000$. More particularly, for the e_1 we chose the flip-rate(p) to be 0.1, and chose $p = 0.2$ for the e_2 . Each image was resized to 14×14 resolution.

For the test evaluation, we randomly sampled 10 instances of p uniformly from the range $[0, 1]$ to construct R_{test} , and approximated the OOD accuracy by computing the worst performance over all R_{test} . We used 5 seeds to produce each numerical result. For the model, we used 4 Layers MLP with 2500 units per each layer and elu activation[9], and did not use bias term in the last sigmoid activation. We used batch normalization (BN)[18] for each layer, and optimized the model using Adam[20] with alpha = 0.0015, beta1=0.0, beta2=0.9 over 500 iterations. In general, less number of iterations yielded better results when $|R_{train}|$ was small (less overfitting).

D.2 Extended Colored MNIST

As described in the main manuscript, Extended Colored MNIST is a modified version of colored MNIST, in which the dataset was constructed using the following procedure. The right panel of the figure 8 is a Bayesian Network representation of this experiment.

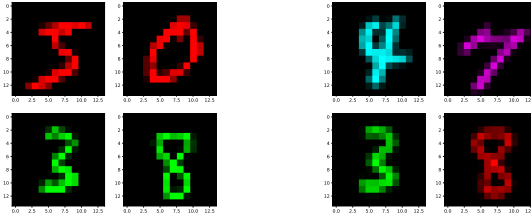
1. Set x_{ch2} to 1 with probability e_{ch2} . Set it to 0 with probability $1 - e_{ch2}$.

2. Construct \hat{y}_{obs} in the same way as in *Colored MNIST*. If $e_{ch2} = k$, construct y_{obs} by flipping \hat{y}_{obs} with probability $p_k (k \in \{0, 1\})$.
3. Put $y_{obs} = \hat{x}_{ch0}$, and construct x_{ch0} from \hat{x}_{ch} by flipping \hat{x}_{ch1} with probability e_{ch0} .
4. Construct x_{obs} as $x_{fig} \times [x_{ch0}, (1 - x_{ch0}), x_{ch2}]$. As an RGB image, this will come out as an image in which the red scale is *turned on* and the green scale is *turned off* if $x_{ch0} = 1$, and otherway around if $x_{ch0} = 0$. Blue scale is turned-on only if $x_{ch2} = 1$.

In this experiment, we set $|R_{train}| = 5$, and choose $|D_e| = 10000$, and resized each image in the dataset to 14×14 resolution. To produce $e \in R_{train}$, we selected e_{ch0} randomly from the range $[0.1, 0.2]$, and selected e_{ch2} randomly from the range $[0.3, 0.4]$.

Mean while, we set $|R_{test}| = 9$. To produce n -th member of R_{test} , we set $e_{ch0} = 0.1$ and we selected e_{ch2} randomly from the range $[0.0, 1.0]$. We chose $p_0 = 0.25, p_1 = 0.75$ for both R_{test} and R_{train} .

We used 5 seeds to produce each numerical result. For the model, we used 4 Layers MLP with 2500 units per each layer, and did not use bias term in the last sigmoid activation. We used batch normalization for each layer, and optimized the model using Adam with alpha = 0.0005, beta1=0.0, beta2=0.9 over 2000 iterations. The performance-values of IRM in the Table 3 of the main article are the results produced by the model that achieved the best average *train* accuracy among all models trained with $\lambda > 10^4$. The averages were computed over 5 seeds.



(a) Example images of *Colored MNIST*. Only two channels are used for all images, and the colors are flipped randomly by the exterior factor.

(b) Example images of *Extended Colored MNIST*. The first two channels and the third channel are perturbed by the different mechanism. See the main manuscript for the way of the construction.

Figure 7: Example of *Colored MNIST* and *Extended Colored MNIST*



Figure 8: The graphical model of *Colored MNIST*(left) and *Extended Colored MNIST*(right)

E Additional Result

The result of *Extended Colored Mnist* with $p_0 = 0.25, p_1 = 0.65$ for both R_{test} and R_{train} . Our algorithm outperforms the Invariant Risk Minimization(IRM)[1] in this case as well in Figure 9.

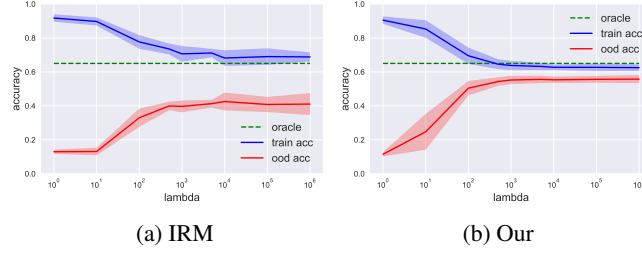


Figure 9: Result on *Extended Colored MNIST* ($p_0 = 0.25, p_1 = 0.65$)

In general, IRM does not work well with standard gradient descent when we implement MLP without Batch Normalization (Figure 10).

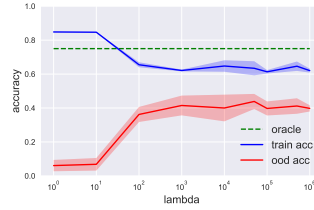


Figure 10: Result on *Colored MNIST* with MLP without BN.

We shall note that the original implementation of the IRM published in Github (<https://github.com/facebookresearch/InvariantRiskMinimization>) uses a very specific schedule for the regularization parameter λ , and it makes λ to jump to a very large value at a very specific timing. The following figures are the result of their original algorithm on MNIST and *Extended Colored MNIST* implemented with various jump-timings of λ . For *Colored MNIST*, the original IRM works for specific choices of the jump timing (200 ~ 300). For *Extended Colored MNIST*, the original algorithm does not work too well for any choice of the jump timings. Meanwhile, IRM works relatively well on *Colored MNIST* consistently if we apply batch normalization, and it works well even without "jumping" the λ . For the tables we present in the main manuscript, we reported the result of IRM implemented *with* batch normalization, which consistently yielded better results than the original implementation.

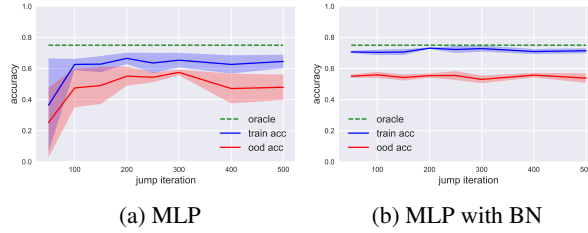


Figure 11: The plot of jump timing against the accuracies on *Colored MNIST*

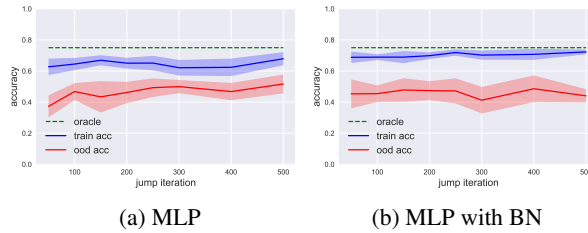


Figure 12: Results on *Extended Colored MNIST*.

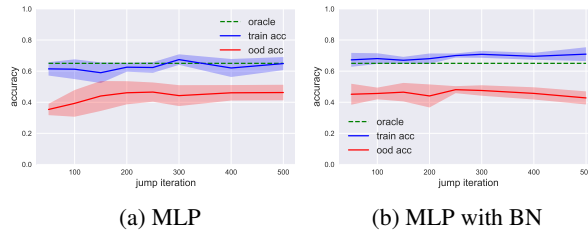


Figure 13: The plot of jump timing against the accuracies on *Extended Colored MNIST*.